

Flavour specific neutrino self-interaction: H_0 tension and IceCube

Arindam Mazumdar^{a,*}, Subhendra Mohanty^{b,†}, Priyank Parashari^{b,c,‡}

a) Centre for Theoretical Studies, Indian Institute of Technology, Kharagpur -721302, India

b) Physical Research Laboratory, Ahmedabad- 380009, India

c) Indian Institute of Technology, Gandhinagar, 382355, India

Abstract

Self-interaction in the active neutrinos is studied in the literature to alleviate the H_0 tension. Similar self-interaction can also explain the observed dips in the flux of the neutrinos coming from the distant astro-physical sources in IceCube detectors. In contrast to the flavour universal neutrino interaction considered for solving the H_0 tension, which is ruled out from particle physics experiments, we consider flavour specific neutrino interactions. We show that the values of self-interaction coupling constant and mediator mass required for explaining the IceCube dips are inconsistent with the strong neutrino self-interactions preferred by the combination of BAO, HST and Planck data. However, the required amount of self-interaction between tau neutrinos (ν_τ) in inverted hierarchy for explaining IceCube dips is consistent with the moderate self-interaction region of cosmological bounds at $1\text{-}\sigma$ level. For the case of other interactions and hierarchies, the IceCube preferred amount of self-interaction is consistent with moderate self-interaction region of cosmological bounds at $2\text{-}\sigma$ level only.

1 Introduction

Self-interaction in between the neutrinos has been an active topic of interest in different sectors of cosmology [1–8], astro-physics [9, 10] and laboratory based neutrino experiments [11–13]. In the recent years it has been studied extensively in the context of resolving H_0 tension [3, 4]. Moreover, if this self-interaction is mediated by some MeV scale boson then the resonant on-shell production of mediator in the collision between the astro-physical neutrinos and the cosmic neutrino background can create some signature in the observed IceCube PeV neutrino flux [14–17]. In this paper we check if these two types of applications of self-interaction in neutrinos are consistent with each other or not.

There is a discrepancy between the determination of the Hubble constant H_0 from Planck [18] (which assumes the Λ CDM cosmology) and those from local measurements based on distance ladder and time delay in lensing observations which points to new physics beyond the Λ CDM model [19–22]. The Planck observation finds the value $H_0 = (67.27 \pm 0.60)$ km/s/Mpc which is in 4.4σ disagreement compared for example to the SHOES collaboration [23] determination of $H_0 = (74.03 \pm 1.42)$ km/s/Mpc, based on the observations by the Hubble Space Telescope of Cepheids in the Large Magellanic Cloud. One of the ways to alleviate the H_0 tension is to have a large self-interaction between neutrinos [3]. Self-interaction delays the free-streaming of neutrinos and neutrinos cluster at smaller length scales. This is compensated by increasing H_0 . In ref. [3] the best fit value of H_0 which is closer to the distance ladder values was obtained by taking an effective neutrino self-interaction $\mathcal{L} = G_{\text{eff}}(\bar{\nu}\nu)(\bar{\nu}\nu)$ with G_{eff} having two preferred values where moderate self-interaction (MI) has $\log_{10}(G_{\text{eff}}\text{MeV}^2) = -3.90^{+1.0}_{-0.93}$ and strong self-interaction (SI) has $\log_{10}(G_{\text{eff}}\text{MeV}^2) = -1.35^{+0.12}_{-0.066}$. In a similar analysis in ref. [4], it is shown that when considering only WMAP data, which measures TT anisotropy spectrum up to multipole $l \leq 1200$, the bimodal peaks in the probability of $\log_{10}(G_{\text{eff}}\text{MeV}^2)$ disappears and neutrino self interactions are consistent with zero. The bimodal distribution of $\log_{10}(G_{\text{eff}}\text{MeV}^2)$ appears when Planck TT and TE data between $1200 \leq l \leq 2500$ are included.

In ref. [3] and [4] (and in earlier studies of CMB with neutrino self-interactions [2], [1]) the neutrino self-interaction that is considered is identical for all neutrino flavours. It has been pointed out that such large flavour universal couplings of neutrinos which implies mediator masses of $\mathcal{O}(\text{MeV})$ is severely constrained from particle physics. Strong bounds on ν self-interactions come from meson decays [12, 24], neutrino-less double beta decay [25] and from Z and τ decays [13]. Neutrino-less double beta decays rule out Majoron mediated ν_e interactions as a solution to

*e-mail: arindam.mazumdar@iitkgp.ac.in

†e-mail: mohanty@prl.res.in

‡e-mail: parashari@prl.res.in

the H_0 tension [25]. Decays of π^+/K^+ to $e^+\nu_e$ and $\mu^+\nu_\mu$ put strong constraints on ν_e and ν_μ interactions while the constraints on ν_τ couplings are determined only from $D_s^+ \rightarrow \tau^+\nu_\tau$ which is not so well constrained [12, 24]. The Z and τ invisible decay width give the strongest bounds for heavy scalar mediators ($m_\phi > 300\text{MeV}$) couplings to ν_τ [13]. To summarize, particle physics allows the self-interactions of ν_τ in the MI region ($m_\phi \sim 10 - 100\text{MeV}$) while universal flavour coupling solution considered in [3, 4] as a solution to the H_0 tension is ruled out [12].

In this paper, we consider flavour specific self-interactions between neutrinos and study their effect on CMB power spectrum. We consider four cases : ν_e, ν_μ, ν_τ and the flavour universal self-interactions. From the CMB analysis we find that there is no discernible difference between the ν_τ self-interactions allowed from particle physics constraints and the universal flavour interactions. We find, similar to the earlier papers [1–4], that $\log_{10}(G_{\text{eff}}\text{MeV}^2)$ has a bimodal distribution in probability with a SI and MI peak. The allowed values of N_{eff} for the joint analysis of Planck CMB, BAO and HST data are significantly higher than three which ensures the larger best-fit values of the Hubble parameter. That is why neutrino self-interactions were considered as a possible solution to the H_0 tension.

Next, we test the flavour specific interactions with IceCube. It has been pointed out that PeV neutrinos from astrophysical sources can interact with cosmic neutrinos and produce an on shell mediator $\nu\nu \rightarrow \phi$, when the neutrino energy $E_\nu = m_\phi^2/(2m_\nu)$ and neutrino self-interactions with MeV mass mediators can have a signature in the neutrino spectrum observed at IceCube [15, 17, 26–30]. The resonant absorption of astrophysical neutrinos will show up as dips in the IceCube flux and this may explain the gap in the IceCube observations between $E_\nu = 400\text{ TeV} - 1\text{ PeV}$ and the non-observation of Glashow-resonance which is expected at $E_\nu = 6.3\text{ PeV}$. Since the neutrino interactions are defined in the flavour basis while the resonance is in the mass basis, the neutrino mixing angles and mass hierarchies also play a crucial role in the IceCube spectrum. We find that all the flavour specific interactions show similar pattern in the IceCube flux data, although these patterns are highly different from the universal interaction. We also find that, for the flavour specific and the universal self-interaction, the cosmological allowed SI region of interaction is ruled out by IceCube data while the MI region is partially consistent with IceCube for both the inverted and normal neutrino mass hierarchies.

The paper is organised as follows. In Section 2 we discuss the models of flavour specific self-interactions and discuss the scattering cross-section in the low energy limit relevant for CMB anisotropy, neutrino free-streaming and the high energy resonant interactions which are relevant for IceCube neutrinos. In Section 3 we discuss the constraints on effective interaction strength (G_{eff}) for the flavour specific and universal interactions from Planck CMB, BAO and HST data. In Section 4 we discuss the propagation of high energy neutrinos in cosmic neutrino background with resonant scattering. In Section 5 we apply the analysis of high energy neutrino propagation to IceCube flux considering the four flavour specific neutrino interactions for the two mass hierarchies. In Section 6 we give our conclusions about the viability of neutrino interaction models for solving the H_0 tension in the light of IceCube data.

2 Self-interaction in neutrinos

Neutrino self-interactions can be mediated by scalars and gauge bosons which are motivated from different particle physics models [31–36]. The lepton number is conserved in the standard model and in the extensions of the standard model where lepton number is broken spontaneously, there are scalars called Majorons which arise from Goldstone bosons of the lepton number symmetry breaking [37]. Neutrino self-interactions can also arise from the gauged lepton number and anomaly free extensions of the standard model where light gauge bosons couple to the neutrinos and evade all other experimental constraints [38]. To analyse the low energy particle physics and CMB constraints, it is enough to work in the effective theory framework [24]. However, to analyse high energy IceCube interactions, where the resonance behaviour of cross-section is needed, the full theory is required.

The neutrino self-interactions are defined in the flavour basis (ν_α) but the high energy propagation and the neutrino free-streaming is analysed in the neutrino mass basis (ν_i). Here Greek letters are for three different flavours e, μ and τ and Latin letters are for mass eigenstates which run from 1 to 3. To relate the couplings in the flavour basis to those in the mass basis, the PMNS mixing matrix defined as

$$|\nu_\alpha\rangle = U_{\alpha i}|\nu_i\rangle, \quad (1)$$

where the values of the components of $U_{\alpha i}$ have been taken from latest NuFit data [39]. Global analysis of the latest neutrino oscillation data provides us the values for all the oscillation parameters like mass squared difference $\Delta m_{ij}^2 = m_i^2 - m_j^2$ and the mixing angles. However, the existing data failed to give the correct sign of Δm_{31}^2 or Δm_{32}^2 . Therefore, we have two mass hierarchies, namely normal hierarchy (NH) and inverted hierarchy (IH). In case of NH

$m_1 < m_2 < m_3$ and in case of IH $m_3 < m_1 < m_2$. For both the hierarchies, we will assume the lowest neutrino mass to be m_0 .

Self-interaction in between the active neutrino species can occur from gauge-interaction or Yukawa like interactions mediated by a scalar(ϕ) particle. In case of Yukawa like interactions the Lagrangian can be written as

$$-\mathcal{L} = g_\phi \sum_{\alpha, \beta} g_{\alpha\beta} \phi \bar{\nu}_\alpha \nu_\beta, \quad (2)$$

where g_ϕ is the coupling strength. In the mass basis this can be written as

$$-\mathcal{L} = g_\phi \sum_{i, j} g_{ij} \phi \bar{\nu}_i \nu_j, \quad (3)$$

where $g_{ij} = g_{\alpha\beta} U_{\alpha i}^* U_{\beta j}$. Similarly for gauge-interactions the Lagrangian can be written as

$$-\mathcal{L} = g_X \sum_{\alpha, \beta} \bar{\nu}_\alpha g_{\alpha\beta} \gamma^\mu P_L \nu_\beta X_\mu, \quad (4)$$

where g_X is the coupling strength. In terms of mass eigenstates this kind of interaction term becomes

$$-\mathcal{L} = g_X \sum_{i, j} g_{ij} \bar{\nu}_i \gamma^\mu P_L \nu_j X_\mu. \quad (5)$$

The matrix $g_{\alpha\beta}$ defines the flavour dependence of the interactions. As discussed earlier, in this paper, we will work with four different types of flavour dependencies. Therefore $g_{\alpha\beta}$ will be $\delta_{\alpha\beta}$ for universal interaction and for interaction in a particular flavour it will be a diagonal matrix with only one among $g_{ee}, g_{\mu\mu}$ or $g_{\tau\tau}$ set to be one.

For both the scalar and vector exchange cases, for momentum-transferred smaller than the mediator mass, the neutrino self-interactions can be described by the four-Fermi term

$$\mathcal{L} = G_{\text{eff}} g_{\alpha\beta} g_{\gamma\delta} \bar{\nu}_\alpha \nu_\beta \bar{\nu}_\gamma \nu_\delta, \quad (6)$$

where $G_{\text{eff}} = g_\phi^2/m_\phi^2$ or $G_{\text{eff}} = g_X^2/m_X^2$ for scalar and gauge boson exchange respectively. For the CMB analysis where the momentum transfer in neutrino scatterings are smaller than MeV^2 , the Four-Fermi effective operator is adequate for the analysis. However, when we consider interactions of high-energy astrophysical neutrinos with the cosmic neutrino background, the effective Four-Fermi interaction is not applicable and one must do the calculations for the full theory with the mediator mass playing a crucial role specially near resonant scattering energies. The high energy neutrino-neutrino scattering cross-section due to scalar exchange is given by [30, 40, 41]

$$\sigma_{ijkl} = \sigma(\bar{\nu}_i \nu_j \rightarrow \bar{\nu}_k \nu_l) = \frac{1}{4\pi} |g_{kl}|^2 |g_{ij}|^2 \frac{g_\phi^4 s_j}{(s_j - m_\phi^2)^2 + m_\phi^2 \Gamma_\phi^2}, \quad (7)$$

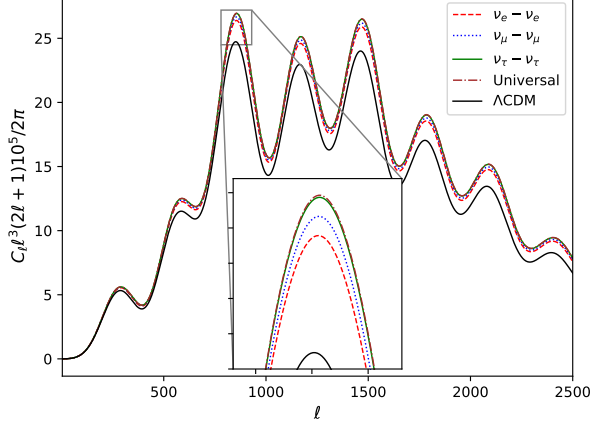
where $s_i = 2E_i m_i$ and $\Gamma_\phi = g_\phi^2 \sum_{i,j} |g_{ij}|^2 m_\phi / 4\pi$ is the decay width of the mediator. For vector interactions the cross-section has the same Breit-Wigner form with different constants in the prefactor. When summed over the final states this turns out to be

$$\sigma_{ij} = \sigma(\bar{\nu}_i \nu_j \rightarrow \bar{\nu} \nu) = \sum_{k,l} \sigma_{ijkl}. \quad (8)$$

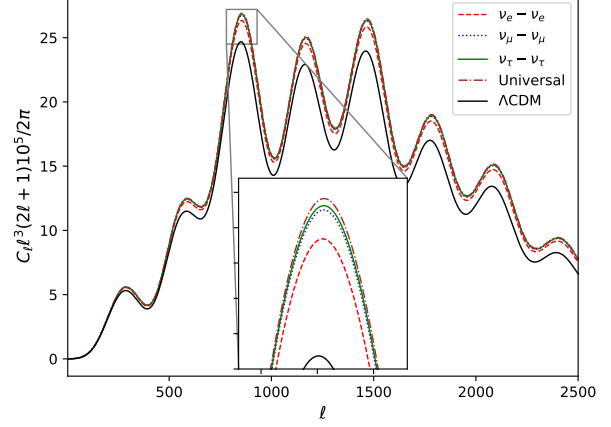
Therefore, we can see that for those energies where s_i becomes equal to the m_ϕ^2 , the scattering cross-section becomes maximum. These energies are called resonant energies and denoted by $E_{Ri} = m_\phi^2 / 2m_i$. In section 4 we will show that corresponding to these resonant energies the absorption rates of astrophysical neutrinos reach the maximum value and we find the dips in the neutrino spectrum in those energy values.

3 Constraints from cosmological data set

We now turn our focus on the cosmological perturbation theory in the presence of self-interaction in massive neutrinos. Massive neutrinos play an important role in the evolution of cosmological perturbations as well as in the evolution of background cosmology. Generally, neutrinos free stream in the baryon-photon fluid of early universe and their free



(a) Normal hierarchy



(b) Inverted hierarchy

Figure 1: Effects of flavour specific interactions on CMB temperature power spectrum are shown. Power spectrum corresponding to universal interaction almost overlaps with that of ν_τ - ν_τ interaction for both the hierarchies. The value of G_{eff} has been fixed to $10^{-1.5} \text{MeV}^{-2}$ for all these cases.

streaming length mainly depends on their masses. However, if the neutrinos have self-interaction in between them then that reduces their free streaming length and makes the neutrinos clump together more and more than the free neutrinos. The mass of the neutrinos on the other hand not only modifies the free streaming length but also modifies the Hubble parameter. That is why the effects of self-interacting neutrinos and the massive neutrinos on CMB are not same. The neutrino interactions are defined in the flavour basis while the neutrino density perturbations are analysed in the mass basis. To study this, we need to calculate the density matrix for the neutrinos which can be written as $\rho_{\alpha\beta} = |\nu_\alpha\rangle\langle\nu_\beta|$ and this transforms to mass basis as

$$\rho_{\alpha\beta} = U_{\alpha i} \rho_{ij} U_{j\beta}^* . \quad (9)$$

Using this we need to find out the Boltzmann hierarchy equations for the massive neutrinos [42] where the collision term is approximated using relaxing time approximation as [43]

$$\frac{1}{\bar{f}_0^i} \frac{\partial f_i}{\partial \tau} = -\frac{\Psi}{\tau_\nu} . \quad (10)$$

Here $\bar{f}_0^i = \sum_\alpha f_0 |U_{\alpha i}|^2 \rho_{\alpha\alpha}$ and f_0 is the zeroth order Fermi-Dirac distribution function [6]. Ψ is the scalar perturbation in the distribution function and τ_ν is the relaxation time which is generally considered as [43]

$$\tau_\nu^{-1} = a n_\nu \langle \sigma v \rangle = \frac{3}{2} \frac{\zeta(3)}{\pi^2} a G_{\text{eff}}^2 T_\nu^5 \rho_{ij} , \quad (11)$$

where T_ν is the neutrino temperature and a is the scale factor. The perturbed Boltzmann equation therefore turns out to be

$$\frac{\partial \Psi_i}{\partial \tau} + i \frac{q(\vec{k} \cdot \hat{n})}{\epsilon} \Psi_i + \frac{d \ln f_0}{d \ln q} \left[\dot{\eta} - \frac{\dot{h} + 6\dot{\eta}}{2} (\hat{k} \cdot \hat{n})^2 \right] = -\Gamma_{ij} \Psi_j , \quad (12)$$

where $\Gamma_{ij} = U^\dagger g_{\alpha\beta} U \tau_\nu^{-1}$. The scalar perturbation Ψ in distribution function is expanded in terms of the Legendre polynomials as, $\Psi(\vec{k}, \hat{n}, q, \tau) = \sum_{\ell=0}^{\infty} (-i)^\ell (2\ell+1) \Psi_\ell(\vec{k}, q, \tau) P_\ell(\hat{k} \cdot \hat{n})$. The individual equations corresponding to the

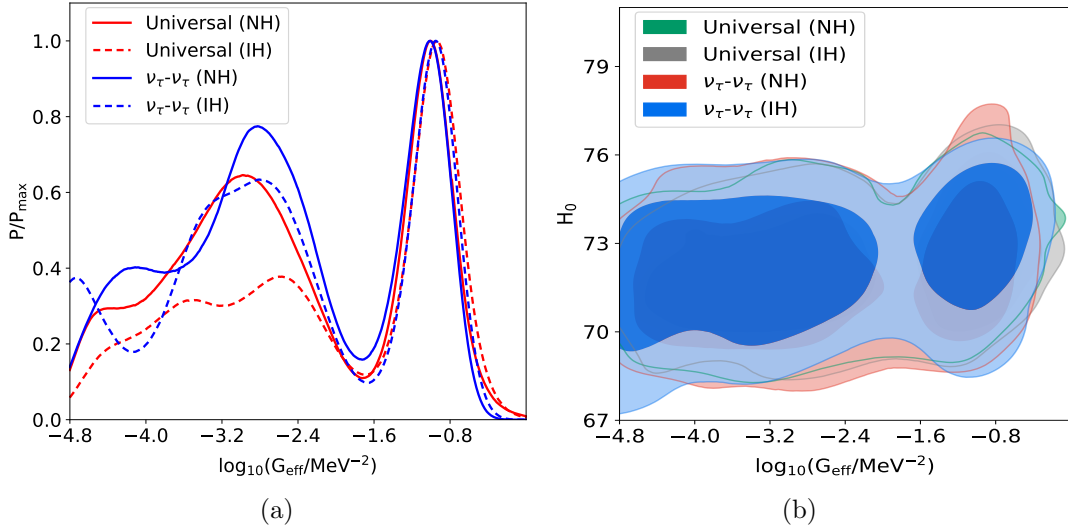


Figure 2: (a) Posterior distribution of G_{eff} is bimodal in nature. (b) Inclusion of self-interaction in the neutrinos resolves H_0 tension as it sets H_0 higher with N_{eff} greater than three when Planck, BAO and HST data analysed jointly. There is no significant effect of hierarchies or the flavour specific nature of the self-interaction on constraining parameters.

multipoles produce the Boltzmann hierarchy equations as follows [44, 45]

$$\dot{\Psi}_{i,0} = -\frac{qk}{\epsilon}\Psi_{i,1} + \frac{1}{6}\dot{h}\frac{d\ln f_0}{d\ln q}, \quad (13a)$$

$$\dot{\Psi}_{i,1} = \frac{qk}{3\epsilon}(\Psi_{i,0} - 2\Psi_{i,2}), \quad (13b)$$

$$\dot{\Psi}_{i,2} = \frac{qk}{5\epsilon}(2\Psi_{i,1} - 3\Psi_{i,3}) - \left(\frac{1}{15}\dot{h} + \frac{2}{5}\dot{\eta}\right)\frac{d\ln f_0}{d\ln q} - \Gamma_{ij}\Psi_{j,2}, \quad (13c)$$

$$\dot{\Psi}_{i,\ell} = \frac{qk}{(2\ell+1)\epsilon}\left[\ell\Psi_{i,(\ell-1)} - (\ell+1)\Psi_{i,(\ell+1)}\right] - \Gamma_{ij}\Psi_{j,\ell} \quad (\ell \geq 3). \quad (13d)$$

Here, the interaction term in the first two equations of eq. (13) was set to zero to conserve the particle numbers and momentum. However, this assumption of conserving particle numbers for a particular mass eigenstate might not hold in case of different values of neutrino masses. According to ref. [46], the exact collision term in first two equations of eq. (13) depends on the differences between the distribution functions of different mass eigenstates. We have checked that this difference is negligible and therefore our assumption of setting the collision terms to zero serves the practical purpose of calculating CMB power spectrum. In a very recent study similar assumption is taken by setting the neutrino masses to zero [47]. We modified these equations (eq. (13)) accordingly in the Boltzmann code CLASS [48] and have shown the effects of these interactions on CMB in fig. (1). In general, self-interaction between neutrinos helps the small scale perturbations to grow therefore the height of the peaks in CMB power spectrum increases. However, the effect of flavour specific interactions on CMB spectrum shows that there are some minor differences between the effects of different interactions. These effects can be understood from the equations 13. In the case of universal interaction when $g_{\alpha\beta}$ is equal to $\delta_{\alpha\beta}$ the Γ_{ij} becomes a diagonal matrix. That means the growth of the scalar perturbation multipoles (Ψ_ℓ) of one mass eigenstate depends only on that mass eigenstate. However, for the case of flavour specific interactions growth of Ψ_ℓ depends on other mass eigenstates too. Ultimately, the amount of the effect of self-interaction is determined by the quantity $\sum_{i,j}\Gamma_{ij}$. In case of universal interaction it is $3\tau_\nu^{-1}$. For ν_e - ν_e interaction this becomes $2.308\tau_\nu^{-1}$, for ν_μ - ν_μ $2.643\tau_\nu^{-1}$ and for ν_τ - ν_τ it turns out to be $2.965\tau_\nu^{-1}$. In case of inverted hierarchy these numbers are $2.309\tau_\nu^{-1}$ for ν_e - ν_e , $2.809\tau_\nu^{-1}$ for ν_μ - ν_μ and $2.88116\tau_\nu^{-1}$ for ν_τ - ν_τ . Therefore, we see that the effects of universal interaction and ν_τ - ν_τ interaction on CMB are almost indistinguishable for both the hierarchies in fig. (1).

We proceed to constrain the parameter space of G_{eff} with Markov Chain Monte Carlo (MCMC) technique using MontePython [49]. We have used the Planck high- ℓ and low- ℓ likelihood, following ref [18, 50] where high- ℓ consists of only TT spectrum and TT, TE and EE spectrum is incorporated in low- ℓ likelihood. We have used two other data

sets. One is baryon acoustic oscillation scale set by BAO-BOSS data of DR12 release [51] and another one is the measured value of H_0 by Hubble space telescope from the observations of Cepheid [23]. We will refer this combined data set as “Planck+BAO+HST”. In this analysis we have varied N_{eff} , lowest neutrino mass m_0 and six standard cosmological parameters. The details of the MCMC is provided in the appendix A. .

As shown in the earlier literature [1–3] we also find that the Planck data along with BAO and HST data prefer a small region of strong interaction between the neutrinos in fig. (2)-(a). The posterior of G_{eff} is bi-modal. For quantifying the two regions of self-interaction we separate out the points from the posterior distribution which have $\log_{10}(G_{\text{eff}})$ values greater than -1.7 and less than that. We use GetDist [52] to extract the statistics of these peaks. The strong interaction region (we call SI onwards) has the value of $\log_{10}(G_{\text{eff}}/\text{MeV}^{-2})$ in one sigma range as $-1.01^{+0.21}_{-0.18}$ for universal interaction in the normal hierarchy, $-0.95^{+0.22}_{-0.18}$ for universal interaction in the inverted hierarchy, $-1.05^{+0.26}_{-0.17}$ for $\nu_\tau\text{-}\nu_\tau$ interaction in the normal hierarchy and $-0.97^{+0.19}_{-0.12}$ for $\nu_\tau\text{-}\nu_\tau$ interaction in the inverted hierarchy. For these specific interactions the bestfit values for $\log_{10}(G_{\text{eff}}/\text{MeV}^{-2})$ in the mildly interacting region (we call MI onwards) are $-3.25^{+0.94}_{-0.65}$, -3.23 ± 0.75 , $-3.20^{+1.3}_{-1.5}$ and $-3.33^{+1.1}_{-0.75}$ respectively. The combined “Planck+BAO+HST” analysis in the case of varying N_{eff} can push the value of H_0 up to 73.3 ± 1.8 in the case of $\nu_\tau\text{-}\nu_\tau$ interaction in normal hierarchy, which resolves the H_0 tension. Similarly for other interactions also the best-fit value of H_0 becomes higher (see fig. (2)-(b)). Values of all other parameters are presented in table 1 and table 2.

In fig. (1) we see that difference in between different types of interactions is almost indistinguishable unless magnified. Even after magnification there is almost no difference in between the effects of $\nu_\tau\text{-}\nu_\tau$ and universal interaction on CMB spectra. Similarly the MCMC bound on G_{eff} for the universal interaction are almost same to the bound in $\nu_\tau\text{-}\nu_\tau$ interaction for both the hierarchies. With these bounds on G_{eff} and m_0 in hand we move forward to calculate the effect of neutrino self-interactions on IceCube flux.

Parameter	Universal Interaction (NH)	Universal Interaction (IH)	$\nu_\tau\text{-}\nu_\tau$ Interaction (NH)	$\nu_\tau\text{-}\nu_\tau$ Interaction (IH)
$10^2\omega_b$	$2.269^{+0.037}_{-0.033}$	2.267 ± 0.035	2.261 ± 0.036	2.266 ± 0.034
ω_{cdm}	$0.1284^{+0.0057}_{-0.0069}$	0.1286 ± 0.0057	$0.1278^{+0.0051}_{-0.0061}$	$0.1280^{+0.0055}_{-0.0067}$
$100\theta_s$	$1.0412^{+0.0009}_{-0.0011}$	$1.0411^{+0.0010}_{-0.0012}$	$1.0413^{+0.0010}_{-0.0011}$	1.0411 ± 0.0010
$\ln(10^{10}A_s)$	3.062 ± 0.037	3.060 ± 0.035	3.058 ± 0.036	3.057 ± 0.035
n_s	0.986 ± 0.014	$0.988^{+0.015}_{-0.013}$	$0.984^{+0.016}_{-0.013}$	$0.986^{+0.015}_{-0.013}$
τ_{reio}	0.057 ± 0.016	0.056 ± 0.015	0.056 ± 0.016	0.056 ± 0.016
m_0	$0.057^{+0.022}_{-0.050}$	$0.058^{+0.025}_{-0.055}$	$0.052^{+0.017}_{-0.049}$	$0.051^{+0.018}_{-0.042}$
$\log_{10} G_{\text{eff}}$	$-3.25^{+0.94}_{-0.65}$	-3.23 ± 0.75	$-3.20^{+1.3}_{-1.5}$	$-3.33^{+1.1}_{-0.75}$
N_{eff}	$3.75^{+0.31}_{-0.38}$	$3.77^{+0.29}_{-0.32}$	$3.69^{+0.28}_{-0.33}$	$3.74^{+0.33}_{-0.37}$
H_0	$72.0^{+1.7}_{-1.9}$	71.8 ± 1.7	71.6 ± 1.8	71.9 ± 1.9

Table 1: $1\text{-}\sigma$ allowed values of all the parameters for the moderate self-interaction interaction for both universal and $\nu_\tau\text{-}\nu_\tau$ interactions.

Parameter	Universal Interaction (NH)	Universal Interaction (IH)	$\nu_\tau\text{-}\nu_\tau$ Interaction (NH)	$\nu_\tau\text{-}\nu_\tau$ Interaction (IH)
$10^2\omega_b$	$2.240^{+0.035}_{-0.041}$	2.248 ± 0.036	2.248 ± 0.040	2.250 ± 0.035
ω_{cdm}	0.1342 ± 0.0064	0.1347 ± 0.0067	$0.1370^{+0.0072}_{-0.0061}$	$0.1366^{+0.0079}_{-0.0049}$
$100\theta_s$	1.0456 ± 0.0012	$1.0454^{+0.0012}_{-0.0014}$	1.0453 ± 0.0011	1.0451 ± 0.0010
$\ln(10^{10}A_s)$	3.003 ± 0.038	$3.004^{+0.030}_{-0.036}$	3.004 ± 0.037	3.009 ± 0.036
n_s	0.959 ± 0.014	0.959 ± 0.013	$0.962^{+0.015}_{-0.011}$	0.964 ± 0.012
τ_{reio}	0.054 ± 0.016	$0.056^{+0.013}_{-0.015}$	$0.050^{+0.014}_{-0.017}$	$0.052^{+0.016}_{-0.014}$
m_0	$0.081^{+0.038}_{-0.069}$	$0.082^{+0.045}_{-0.054}$	$0.084^{+0.044}_{-0.060}$	0.092 ± 0.062
$\log_{10} G_{\text{eff}}$	$-1.01^{+0.21}_{-0.18}$	$-0.95^{+0.22}_{-0.18}$	$-1.05^{+0.26}_{-0.17}$	$-0.97^{+0.19}_{-0.12}$
N_{eff}	3.93 ± 0.35	3.97 ± 0.36	$4.07^{+0.39}_{-0.35}$	$4.09^{+0.42}_{-0.21}$
H_0	72.8 ± 1.9	72.9 ± 1.7	73.3 ± 1.8	$73.3^{+2.0}_{-1.4}$

Table 2: $1\text{-}\sigma$ allowed values of all the parameters for the strong self-interaction interaction for both universal and $\nu_\tau\text{-}\nu_\tau$ interactions.

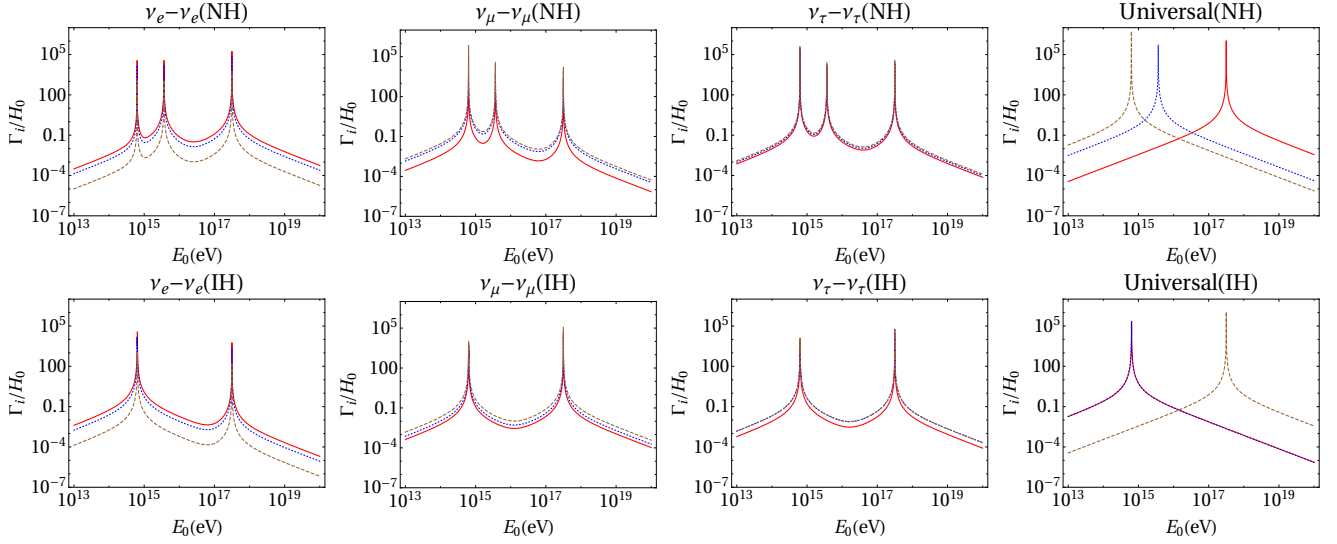


Figure 3: Effects of different types of interaction on absorption rate (Γ_i) are shown. Red, blue (dotted) and brown (dashed) line demonstrate the interaction rates corresponding to mass eigenstates 1,2 and 3 respectively. Here, the upper panel represents normal hierarchy and the lower panel represents inverted hierarchy. Values of the parameters for these plots kept fixed at $m_\phi = 10^{6.9}\text{eV}$, $g_\phi = 10^{-1.5}$ and $m_0 = 10^{-4}\text{eV}$.

4 Neutrino absorption by Cosmic Neutrino Background

Propagation of the astrophysical neutrinos in the cosmic neutrino background can be described by the Boltzmann equation. The specific flux Φ_i of neutrino mass eigenstates m_i is defined as

$$\Phi_i = \frac{\partial n_i}{\partial E}, \quad (14)$$

where n_i is the comoving number density of the astrophysical neutrinos per unit time and E is the energy of the neutrino mass eigenstates. Therefore, the unit of the Φ_i is $\text{cm}^{-2}\text{s}^{-1}\text{sr}^{-1}\text{eV}^{-1}$. The Boltzmann equation for Φ_i is defined as [14, 41]

$$\frac{\partial \Phi_i}{\partial t} = H\Phi_i + HE\frac{\partial \Phi_i}{\partial E} + S_i(t, E) - \Gamma_i(t, E)\Phi_i + S_{\text{tert},i}(t, E). \quad (15)$$

Here, H denotes the Hubble parameter, S_i is the source term of the astrophysical neutrinos, Γ_i is absorption rate and $S_{\text{tert},i}$ is the tertiary source term. Absorption rate $\Gamma_i = \sum_j \tilde{n}_j \sigma_{ij}$, where \tilde{n}_j is the comoving cosmological neutrino number density [30]. Absorption rate is plotted against energy in fig. (3), we can see that Γ_i becomes maximum at the resonance energies. For solving eq. (15), we recast it in redshift (z) variable as

$$(1+z)\frac{\partial \Phi_i}{\partial z} + E\frac{\partial \Phi_i}{\partial E} = -\Phi_i - \frac{S_i(z, E)}{H} + \frac{\Gamma_i(z, E)}{H}\Phi_i - \frac{S_{\text{tert},i}(z, E)}{H}. \quad (16)$$

Solution of this equation is done using method of auxiliary equation [14, 41], where the auxiliary equation is set to be

$$E = E_0(1+z). \quad (17)$$

Here E_0 denotes the energy of neutrinos at $z = 0$. The solution of eq. (16) can be written as [53]

$$\Phi_i(E_0, z) = \int_0^\infty \frac{dz'}{H(z')} \exp \left[\int_z^{z'} \frac{dz''}{(1+z'')} \frac{\Gamma_i(E, z'')}{H(z'')} \right] \{S_i(E, z) + S_{\text{tert},i}(E, z)\}. \quad (18)$$

The source term S_i is mainly the astrophysical neutrinos generated from the core-collapsed supernova (CCSN). Therefore this term is taken as [54]

$$S_i(t, E) = R_{\text{CCSN}}(z) \frac{dN_i}{dE} E^{-\gamma}, \quad (19)$$

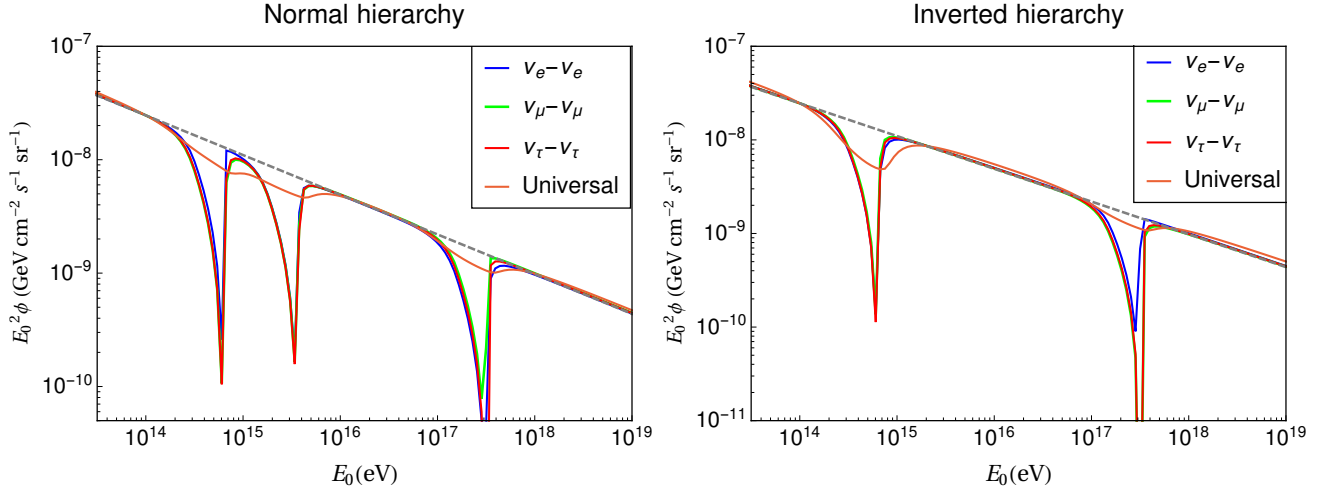


Figure 4: Effects of different types of self-interaction on total neutrino flux for both hierarchies are shown. Values of the parameters for these plots kept fixed at $m_\phi = 10^{6.9}\text{eV}$, $g_\phi = 10^{-1.5}$, $\gamma = 2.35$ and $m_0 = 10^{-4}\text{eV}$. Dashed line corresponds to $\Phi \propto E_0^{-\gamma}$.

where $\frac{dN_i}{dE}$ is the comoving neutrino production rate per unit time per unit energy and it is defined as

$$\frac{dN_i}{dE} = \frac{120E^2 E_{\text{tot}}}{(7\pi^2) 6(k_B T_{\text{sn}})^4 (e^{E/k_B T_{\text{sn}}} + 1)}, \quad (20)$$

where $E_{\text{tot}} = 1.873 \times 10^{65}\text{eV}$ and $k_B T_{\text{sn}} = 8\text{ MeV}$ [30].

$R_{\text{CCSN}}(z)$ represents the number density of the core-collapsed supernova as a function of z . We take this function from ref [55]

$$R_{\text{CCSN}}(z) = \dot{\rho} \left(\left(\frac{z+1}{B} \right)^{\beta\eta} + \left(\frac{z+1}{C} \right)^{\gamma_2\eta} + (z+1)^{\alpha\eta} \right)^{1/\eta} \quad (21)$$

with the parameters being $\dot{\rho} = 0.0178$, $z_1 = 1$, $z_2 = 4$, $\alpha = 3.4$, $\beta = -0.3$, $\gamma_2 = -3.5$, $\eta = -10$, $B = (z_1 + 1)^{1-\frac{\alpha}{\beta}}$ and $C = (z_2 + 1)^{1-\frac{\beta}{\gamma_2}} (z_1 + 1)^{\frac{\beta-\alpha}{\gamma_2}}$.

Tertiary source term, $S_{\text{tert},i}$ accounts for the up-scattering of the cosmological neutrinos from the collision with astrophysical neutrinos. This term is approximated in the literature in many different ways. In this paper we use the form provided by ref [30] which is

$$S_{\text{tert},i}(z, E) = \sum_{jkl} (1 + \delta_{il}) \tilde{n}_k(z) \sigma_{jkl} \Phi_j(z, E_{R_k}) \Theta(E_{R_k} - E). \quad (22)$$

We have computed the specific flux of neutrino at $z = 0$ by numerically solving eq. (18). We have taken the maximum value of z in this equation to be 10. It is because the $R_{\text{CCSN}}(z)$ function has non-negligible value up to redshift ten. Normalization of the $E_0^2 \sum_i \Phi_i$ is fixed to $2.46 \times 10^{-8} \text{GeV cm}^{-2} \text{s}^{-1} \text{sr}^{-1}$ for neutrino energy equal to 100 TeV [56]. The results for different types of interactions and hierarchies are shown in fig. (4). To understand these plots we have made another set of plots in fig. (3) where the values of absorption rate, Γ_i has been plotted for different interactions. We see that there is a major difference between the universal interaction and the flavour specific interactions. In case of universal interaction the g_{ij} and g_{kl} in eq. (7) becomes kronekar delta function and thus Γ_i gets the contribution from s_i only. However, for flavour specific interactions g_{ij} mixes all the mass eigenstates and s_j corresponding to all mass eigenstates contributes in Γ_i . Therefore, in fig. (3) we see that for flavour specific interactions the Γ_i shows resonance peaks in all three possible energy values corresponding to the three mass eigenstates in normal hierarchy. In the case of inverted hierarchy the mass gap between first two mass eigenstates are small, and the peaks corresponding to those mass eigenstates are indistinguishable, therefore, only two peaks are separately visible. These peaks in Γ_i leads to the absorption dips in the flux of astrophysical neutrinos in fig. (4). Since, in the case of flavour specific interactions all mass eigenstates undergo absorption in all dips (three

dips for NH and two dips for IH), we see that the total flux also shows dips in all the resonance energies. However, in the case universal interaction in which energy one mass eigenstate undergoes resonant absorption other mass eigenstates do not. Therefore, in fig. (4) the universal curve shows a more flat line. The three different peaks in the Γ_i of universal interaction can come close together if neutrino masses become degenerate. In that case a prominent dip will be visible in the total neutrino flux for universal interaction also. However, that means it requires a higher value lowest neutrino mass and in the next section we will check if that is consistent with CMB bound.

We found that the contribution of the tertiary source term compared to the core-collapse supernova source term is negligibly small. Moreover, it considerably increases the computation time. Therefore, for constraining the parameter space using IceCube data we neglect the tertiary term in the next section.

5 Parameter estimation from flux at IceCube

In IceCube six-year HESE data, 82 events passed the selection criterion of which two are coincident with atmospheric muons and left out. The best fit for single power law flux is [56]

$$E_0^2 \phi = (2.46 \pm 0.8) \times 10^{-8} \left(\frac{E_0}{100 \text{ TeV}} \right)^{-0.92} \text{ GeV cm}^{-2} \text{ s}^{-1} \text{ sr}^{-1}, \quad (23)$$

which has a softer spectral index than the 3-year ($\gamma = 2.3$) as well as the 4-year ($\gamma = 2.58$) data. These events are binned in 6 values of energy and for other values of energy where no events have been observed, an upper bounds on the neutrino flux have been provided. For fitting our numerical results of flux with the IceCube data we have solved eq. (18) for 63 different values of E_0 which are equally spaced in log scale within E_0 -range of first 7 points in IceCube data (see fig. (5)). Therefore, we have sampled each energy bin with 9 points in the log scale. The average of these 9 points are assigned as the theoretical prediction of neutrino flux. These theoretical predictions are then compared to the observational values of binned flux and the allowed parameter space (m_ϕ , g_ϕ , m_0 and γ) has been estimated using the MCMC technique with Metropolis-Hastings algorithm. Please refer to the appendix A for details.

Before moving forward to describe our findings for different types of interactions and hierarchies, let us briefly summarize the effects of different parameters on the features of the specific flux of neutrinos in IceCube. These effects can be listed as

- The higher value of m_ϕ shifts the dips towards the higher values of neutrino energy.
- The higher values of lowest neutrino mass m_0 make the difference between the neutrino masses smaller and thus make absorption dips come closer.
- In case of universal interaction higher m_0 makes dips sharper and lower m_0 makes the flux more flat.
- In general, higher values of m_0 make the neutrinos heavier and therefore the dips move towards lower values of neutrino energy.
- Higher values of g_ϕ make the dips sharper.
- γ determines the slope of the flux line. The more γ becomes close to the value 2 the more the flux line becomes flat.

In the next subsections we will discuss our findings of MCMC analysis of parameter space for both the hierarchies and different types of interactions.

5.1 Normal hierarchy

Universal interactions: Number of visible dips in the neutrino specific flux heavily depends on the value of the lowest neutrino mass m_0 . Moreover, as shown in the fig. (4) the universal interaction produces more flat line of specific flux compared to the flavour specific interactions for smaller values of m_0 . However, when the m_0 is large, the absorption dips in flux lines corresponding to the different mass eigen states come closer and the dips in the total flux become sharper. Therefore, to fit the dips in the IceCube data the universal interaction prefers a higher value of m_0 . The bestfit values along with $1-\sigma$ error for all the parameters (m_ϕ , g_ϕ , γ and m_0) are given in table 3. Moreover, the cosmological $1-\sigma$ upper bound of m_0 for the case of moderate universal interactions in the normal

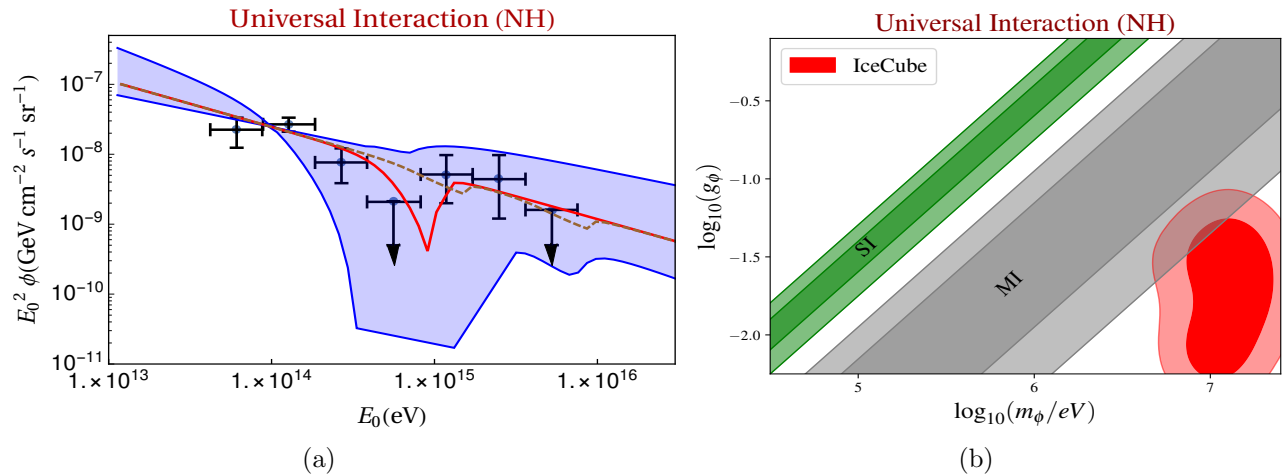


Figure 5: **Universal interaction in normal hierarchy:** (a) The shaded region corresponds to the specific flux of the neutrinos allowed by the 1- σ ranges of all the parameters (m_ϕ , g_ϕ , γ and m_0) as given in table 3. The solid red line corresponds to the bestfit values of all these parameters. However, the orange dashed line corresponds to parameters m_ϕ , g_ϕ and γ fixed at their bestfit values and m_0 value fixed at zero. (b) The allowed 1- σ and 2- σ regions in the m_ϕ - g_ϕ plane from IceCube data are shown along with the cosmological bound (“Planck+BAO+HST”) for universal interaction in the normal hierarchy. The allowed region for IceCube has no overlap with the strong self-interaction (SI) band.

hierarchy is 0.079 eV (see table 1). The disallowed values of m_0 are shown as the green shaded region in fig. (7)-(a). Therefore, It is clear from fig. (7)-(a) that a substantial region of the preferred mass range by IceCube is disallowed by the cosmological bound.

In fig. (5), the specific flux in IceCube and the corresponding allowed parameter space for m_ϕ - g_ϕ have been shown. The shaded region in the fig. (5)-(a) corresponds to the specific flux of the neutrinos by the maximum allowed values of all the parameters (m_ϕ , g_ϕ , γ and m_0) within the 1- σ range. The shaded region shows that the dip in the specific flux can reach only up to a certain minima and it cannot go deeper since that will require larger neutrino masses than the specified upper bound on m_0 in table 3. We have also plotted a red solid line and a dashed orange line of the specific flux. The red solid line corresponds to bestfit values of all the parameters. Whereas, the orange line corresponds to the $m_0 = 0$ eV and all other parameters m_0 , g_ϕ and γ fixed to their best-fit values. As discussed in the previous section, “Planck+BAO+HST” data also puts a bound on G_{eff} , which translate into a bound on m_ϕ - g_ϕ parameter space. The 1- σ and 2- σ bounds for both SI and MI region have been shown by the green and gray shaded area respectively in fig. (5)-(b). It is quite evident from fig. (5)-(b) that the IceCube allowed parameter space for m_ϕ - g_ϕ is inconsistent with SI bound. Whereas, some part of IceCube allowed parameter space for m_ϕ - g_ϕ overlaps with MI bound at 2- σ level only.

ν_τ - ν_τ interactions: The main difference in the features of flavour specific interaction and universal interaction is that while flavour specific interaction can produce two prominent dips in two different energy bins of IceCube data, the universal interaction allows only one prominent dip. However, the two dips in a flavour specific interaction can be merged to one by increasing the neutrino mass. The bestfit values along with 1- σ error for all the parameters (m_ϕ , g_ϕ , γ and m_0) is given in table 3. The specific flux of the neutrinos corresponds to the 1- σ allowed values of all these parameters is shown by the shaded region in the fig. (6)-(a). We have also plotted two different lines, the solid red and orange dashed line, for specific flux in IceCube which show quite different features. For the orange dashed line, m_0 has been taken to be zero and all other parameters has been kept at their best fit values. This line can explain two dips in IceCube data at two different energies. If the neutrino mass is increased, the orange dashed line in the figure moves towards the solid red line which corresponds to the bestfit values of all the parameters presented in table 3. Therefore we see in the fig. (6)-(a) that the solid red line and the orange dashed line represent the one and two dip solutions in the IceCube energy range. Similar to the universal case, it is quite evident from fig. (6)-(b) that the IceCube allowed parameter space for m_ϕ - g_ϕ is inconsistent with SI region. Whereas, IceCube allowed parameter space for m_ϕ - g_ϕ is consistent with MI bound at 2- σ level. We have also presented the IceCube allowed parameter space for m_ϕ - m_0 in fig. (7)-(b). The cosmological 1- σ upper bound of m_0 is 0.069 eV for moderate ν_τ - ν_τ interaction

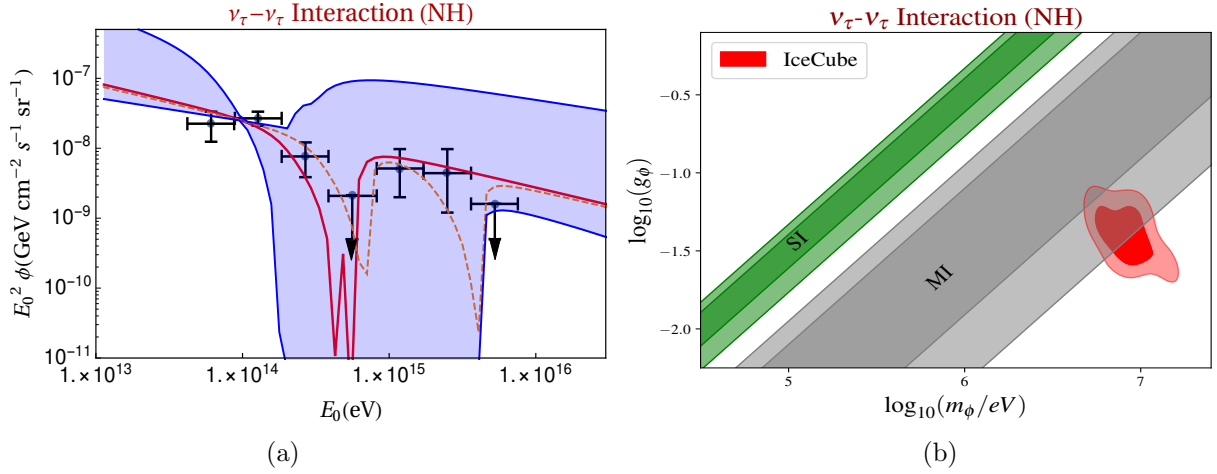


Figure 6: ν_τ - ν_τ **interaction in normal hierarchy**: (a) The shaded region corresponds to the specific flux of the neutrinos allowed by the 1- σ ranges of all the parameters in table 3. The solid red line correspond to the best fit values of all the parameters and the orange dashed line corresponds to the best fit value of m_ϕ , g_ϕ and γ and the value of m_0 is fixed at zero. (b) The allowed 1- σ and 2- σ regions in the m_ϕ - g_ϕ plane from IceCube data are shown along with the bounds from the cosmological bound (“Planck+BAO+HST”) for ν_τ - ν_τ interaction in the normal hierarchy. The allowed region for IceCube has no overlap with the strong self-interaction (SI) band.

Parameter	68% limits
<u>Universal interaction</u>	
$m_0(\text{eV})$	$0.067^{+0.038}_{-0.046}$
$\log_{10}(m_\phi/\text{eV})$	7.09 ± 0.15
$\log_{10} g_\phi$	-1.75 ± 0.31
γ	$2.66^{+0.21}_{-0.18}$
<u>ν_τ-ν_τ interaction</u>	
$m_0(\text{eV})$	$0.062^{+0.042}_{-0.046}$
$\log_{10} m_\phi/\text{eV}$	6.92 ± 0.11
$\log_{10} g_\phi$	-1.40 ± 0.13
γ	2.50 ± 0.17

Table 3: The preferred bestfit values of the IceCube parameters and their 1- σ ranges for both universal and ν_τ - ν_τ interaction case in the **normal hierarchy**. are listed in this table

in case of normal hierarchy. The disallowed region is shown in the green color in fig. (7)-(b), which rules out a substantial part of IceCube allowed m_0 values.

5.2 Inverted Hierarchy

Universal interactions: Similar to the case of normal hierarchy, in the case of inverted hierarchy, the universal interaction produces a flatter specific flux line compared to the the flavour specific interactions for smaller values of m_0 as well. Since large values of m_0 make masses of different neutrino mass eigenstates almost degenerate, we get a single dip solution for such case. Therefore, again to fit the dips in the IceCube data the universal interaction prefers a higher value of m_0 . The bestfit values along with 1- σ error for all the parameters (m_ϕ , g_ϕ , γ and m_0) are given in table 4. “Planck+BAO+HST” data also put a bound on the lowest neutrino mass $m_0 \leq 0.083$ eV for the moderate universal interaction in the inverted hierarchy. The values of m_0 excluded by the cosmological data are shown in the green shaded region in fig. (10), which clearly implies that a substantial fraction of the IceCube preferred mass range is disallowed by the cosmological bound.

In fig. (8), the specific flux in IceCube and the corresponding allowed parameter space for m_ϕ - g_ϕ have been shown. The shaded region in the fig. (8)-(a) corresponds to the specific flux of the neutrinos for the maximum allowed values of all the parameters (m_ϕ , g_ϕ , γ and m_0) within the 1- σ range. Similar to the normal hierarchy case, the shaded region shows that the dip in the specific flux can reach only up to a certain minima and it cannot go deeper cause

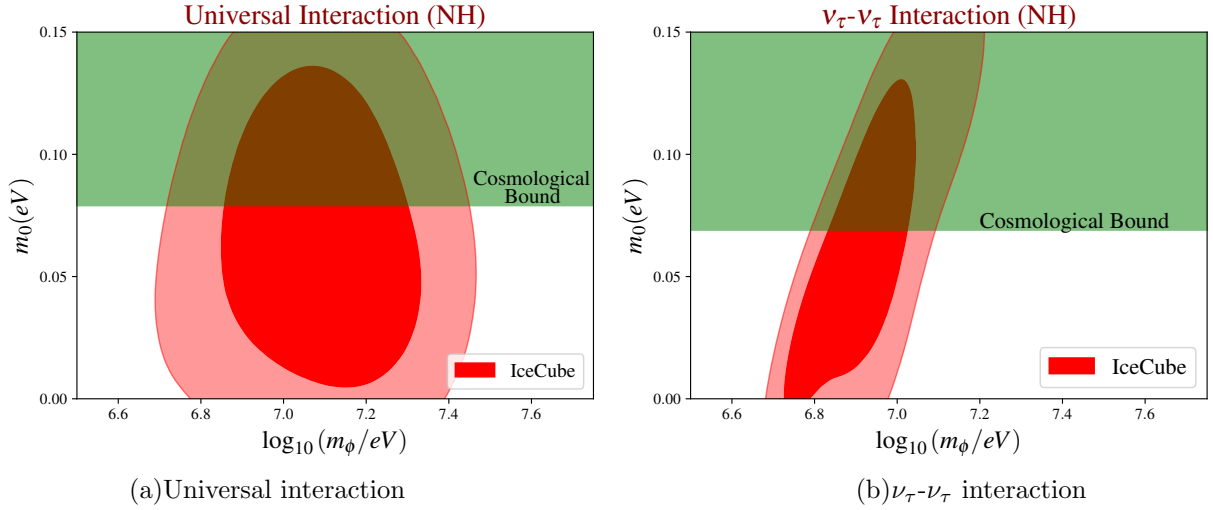


Figure 7: The green region shows the values of lowest neutrino mass (m_0) excluded by cosmological data (“Planck+BAO+HST”) for the normal hierarchy. A major portion of the preferred m_0 values by IceCube data is disfavored by the cosmological bound.

that will require larger neutrino masses. We have also plotted a red solid line and a dashed orange line of specific flux. The red solid line corresponds to the best fit values of all the parameters listed in table 4. Whereas, the orange line corresponds to the $m_0 = 0$ eV and all other parameters fixed at their best fit values. Similar to the normal hierarchy, It is quite evident from fig. (8)-(b) that the IceCube allowed parameter space for m_ϕ - g_ϕ is inconsistent with SI bound. However, some part of IceCube allowed parameter space for m_ϕ - g_ϕ overlaps with MI bound at 2- σ level only.

ν_τ - ν_τ interactions: In case of inverted hierarchy, for the ν_τ - ν_τ interaction, number of dips in the IceCube energy range depends on the m_0 value. For very small value of m_0 (close to zero) we get one dip in the IceCube energy range. Similarly, in the case of larger values of m_0 , when all the three mass eigenstates become almost degenerate, we find only one dip in the IceCube energy range. On the other hand, for the values of m_0 , which are not very close to zero and also not very large to make all three mass eigenstates degenerate, we can get two dips in the IceCube energy range. The bestfit values along with 1- σ error for all the parameters (m_ϕ , g_ϕ , γ and m_0) are given in table 4. In fig. (9), the specific flux in IceCube and the corresponding allowed parameter space for m_ϕ - g_ϕ have been shown. We have also plotted three different lines, the solid red, orange dashed and dotted pink line, for the specific flux in IceCube which show very different features. The orange dashed line is for $m_0 = 0$ eV and all other parameters are fixed at their best fit values. We can see from the fig. (9)-(a) that this line represents the one dip solution. As we increase the m_0 value, the orange dashed line moves towards the pink dotted line. In case of the pink dotted line,

Parameter	68% limits
Universal interaction	
$m_0(\text{eV})$	$0.052^{+0.034}_{-0.040}$
$\log_{10}(m_\phi/\text{eV})$	6.883 ± 0.091
$\log_{10} g_\phi$	-1.87 ± 0.20
γ	2.63 ± 0.17
ν_τ-ν_τ interaction	
$m_0(\text{eV})$	$0.062^{+0.038}_{-0.058}$
$\log_{10}(m_\phi/\text{eV})$	$6.936^{+0.089}_{-0.14}$
$\log_{10} g_\phi$	-1.25 ± 0.17
γ	$2.46^{+0.18}_{-0.16}$

Table 4: The preferred bestfit values of the IceCube parameters and their 1- σ ranges for both universal and ν_τ - ν_τ interaction case in the **inverted hierarchy**. are listed in this table.

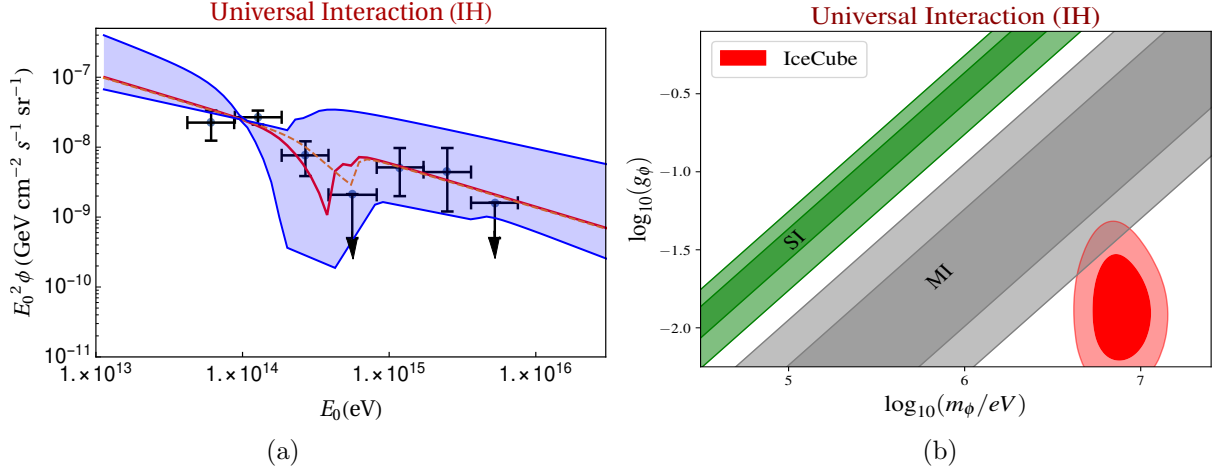


Figure 8: **Universal interaction in inverted hierarchy:** (a) The shaded region corresponds to the specific flux of the neutrinos allowed by the $1\text{-}\sigma$ ranges of the parameters in table 4. The solid red line correspond to the best fit values of the parameters and the orange dashed line corresponds to the best fit value of m_ϕ, g_ϕ and γ (in table 4) and the value of m_0 is fixed at zero. (b) The allowed $1\text{-}\sigma$ and $2\text{-}\sigma$ regions in the m_ϕ - g_ϕ plane from IceCube data are shown along with the cosmological bound ("Planck+BAO+HST") for universal interaction in the inverted hierarchy. The allowed region for IceCube has no overlap with the strong self-interaction (SI) band.

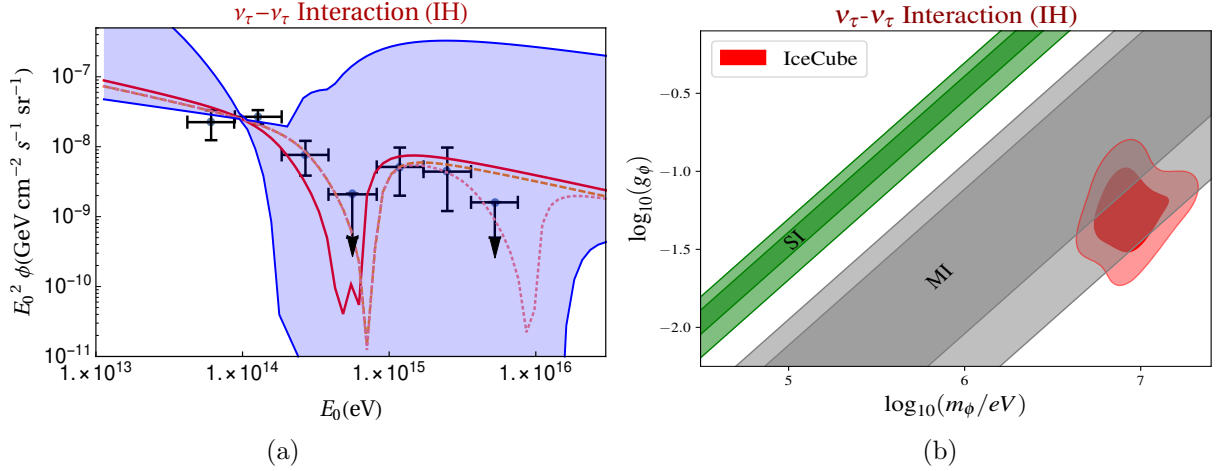


Figure 9: **ν_τ - ν_τ interaction in inverted hierarchy:** (a) The shaded region corresponds to the specific flux of the neutrinos allowed by the $1\text{-}\sigma$ ranges of all the parameters in table 4. The values of m_ϕ, g_ϕ and γ has been fixed to their bestfit values (in table 4) for all the solid red line, orange dashed line and the pink dotted line. However, the solid red line corresponds to the bestfit value of m_0 ; the orange dashed line corresponds to the m_0 value fixed at zero and the pink dotted line corresponds to the lowest $1\text{-}\sigma$ allowed value of m_0 . (b) The allowed $1\text{-}\sigma$ and $2\text{-}\sigma$ regions in the m_ϕ - g_ϕ plane from IceCube data are shown along with the cosmological bound ("Planck+BAO+HST") for ν_τ - ν_τ interaction in the inverted hierarchy. The allowed region for IceCube has no overlap with the strong self-interaction (SI) band.

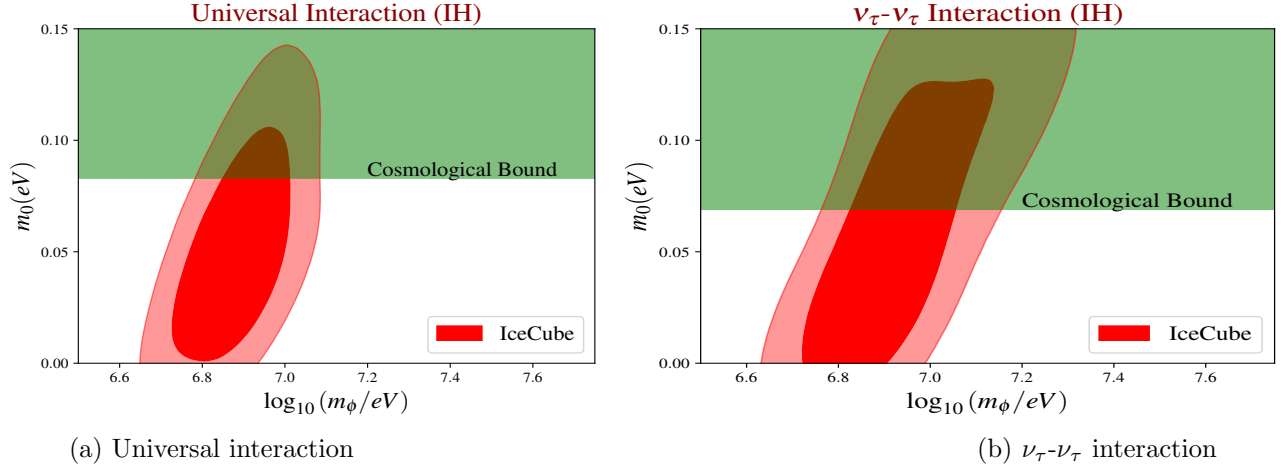


Figure 10: The green region shows the values of lowest neutrino mass (m_0) excluded by cosmological data (“Planck+BAO+HST”) for the inverted hierarchy. For both the interaction cases, a significant portion of the preferred m_0 values by IceCube data is excluded by the cosmological bound.

we have kept the value of m_0 fixed at lowest 1- σ value. It can be clearly seen from the fig. (9)-(a) that pink dotted line can explain two dips in IceCube data at two different energies. If the neutrino mass is increased further the pink dotted line moves towards the solid red line which corresponds to the bestfit values of the all parameters presented in table 4. Therefore, we can clearly see from the fig. (9)-(a) that the solid red and orange dashed line represent the one dip solutions in the IceCube energy range, whereas the pink dotted line represents the two dip solution. The shaded region in the fig. (9)-(a) corresponds to the specific flux of the neutrinos for the maximum allowed values of all the parameters (m_ϕ, g_ϕ, γ and m_0) within the 1- σ . Once again, It is quite evident from fig. (9)-(b) that the IceCube allowed parameter space for m_ϕ - g_ϕ is inconsistent with SI bound. However, IceCube allowed parameter space for m_ϕ - g_ϕ is consistent with MI bound at 1- σ level. We have also presented the IceCube allowed parameter space for m_ϕ - m_0 in fig. (10)-(b). The 1- σ maximum value of m_0 allowed by “Planck+BAO+HST” data is 0.069 eV for moderate ν_τ - ν_τ interaction in case of inverted hierarchy. This cosmological disallowed region is shown in the green shade in fig. (7)-(b) which implies that a substantial part of IceCube allowed m_0 values is ruled out by the cosmological bound.

6 Conclusions

In this paper we have studied the self-interaction between the neutrinos in the context of H_0 tension and the observed dips in the neutrino flux at IceCube. We have shown that the flavour specific interaction and the universal interaction does not affect CMB power spectrum very much differently. Even the inverted hierarchy and the normal hierarchy do not have much distinguishable effect. The bound on the self interaction parameter G_{eff} from the “Planck+BAO+HST” data shows a bimodal feature in its distribution which is consistent with the earlier studies. The bestfit values of G_{eff} from the MCMC analysis are also similar for different types of interaction in different hierarchies. Without self-interaction in neutrinos the maximum allowed value of N_{eff} does not increase the value of H_0 to the level of resolving H_0 -tension [18]. Whereas, the inclusion of self-interaction increases the bestfit value of N_{eff} and help to resolve the H_0 tension.

The effect of the flavour specific and the universal interaction on the total flux of astrophysical neutrinos in IceCube is quite different. We have plotted different ways of fitting IceCube data with these interactions and constrained the parameter space of self-interaction mediator and the neutrino mass. We find that the dips in between 400 TeV -1 PeV and at around 6 PeV (which shows the non-appearance of Glashow resonance) can be simultaneously explained using the neutrino self-interaction in flavour specific cases. However, in case of universal interaction it is impossible to explain two dips simultaneously and by adjusting the parameters, only one dip can be explained. Moreover, by suitably adjusting the lowest neutrino mass, two different dips in flavour specific cases can also be merged into a single dip. We find that there is no distinguishable difference in the features of the neutrino flux line for ν_e - ν_e , ν_μ - ν_μ and ν_τ - ν_τ interaction. Therefore, all the analysis and the results presented here for the ν_τ - ν_τ interaction are equally applicable to the ν_e - ν_e and ν_μ - ν_μ interaction cases.

Hierarchies also play an important role in determining the position and the shape of the absorption dips in the neutrino flux at IceCube. In the case of universal interaction and normal hierarchy, two very small dips can occur for lowest neutrino mass being zero. However, for the same case in the inverted hierarchy there can be only one small dip if m_0 is fixed at zero. In case of ν_τ - ν_τ interaction, normal hierarchy can produce two dips in the above mentioned two energy values (around 500 TeV and 6 PeV) for the value of m_0 fixed at zero. However, in case of inverted hierarchy that same feature requires small but non zero lowest neutrino mass.

Since, the value of mediator mass (m_ϕ) changes the position of the dips and the value of the interaction strength (g_ϕ) changes the sharpness of the dips, the MCMC analysis provide quite strict bound on those values. Larger values of g_ϕ beyond the obtained bound can produce sharper dips in the resonance energies, but it will not be able to explain the absorption feature throughout the specified energy range of a certain bin in the IceCube data. We found that the cosmological bound on the neutrino self-interaction parameters in strong interaction (SI) region, which are inferred from the joint analysis of Planck, HST and BAO data, are inconsistent with the parameter space inferred from the IceCube data. The preferred parameter space of g_ϕ - m_ϕ by the IceCube data can only be slightly consistent with the moderate interaction (MI) allowed by the cosmological data set. More specifically, only the ν_τ - ν_τ interaction in the inverted hierarchy prefers g_ϕ - m_ϕ parameter space that is in 1- σ concordance with cosmological constraints. For all other cases of neutrino self-interactions studied in this paper allowed parameter space from IceCube data and cosmological data matches at 2- σ level only. We have also plotted the allowed region of flux line beyond 10 PeV neutrino energy in our results. Therefore, it serves as a prediction for upcoming data in IceCube experiment in ultra high energies.

Acknowledgment

We acknowledge the computation facility, 100TFLOP HPC Cluster, Vikram-100, at Physical Research Laboratory, Ahmedabad, India.

Appendix

A Numerical details

The MCMC analysis performed in the paper for the IceCube data is based upon the Metropolis-Hastings algorithm [57]. The likelihood function used in the analysis assumes a generalized likelihood function for asymmetric error, following ref. [58] which can be written as

$$\ln[L] = \sum -\frac{1}{2} \left(\frac{\hat{x} - x}{\sigma + \sigma'(\hat{x} - x)} \right)^2, \quad (24)$$

where,

$$\sigma = \frac{2\sigma_+\sigma_-}{\sigma_+ + \sigma_-} \text{ and } \sigma' = \frac{\sigma_+ - \sigma_-}{\sigma_+ + \sigma_-}, \quad (25)$$

with σ_+ and σ_- are the positive and negative errors. In case of symmetric errors $\ln[L]$ turns out to be $-\chi^2$. In the likelihood function we used the binned flux data of ref. [56] as observational values. Theoretical values are calculated from the solution of eq. (18) for 63 different points in the IceCube energy range where we have taken 9 points from each bin in equally spaced log space of E_0 .

We have used the Gaussian priors for all the parameters and the corresponding values are given table 5. We have also set the maximum and minimum values at 7.4 and 6.2 respectively for $\log_{10}(m_\phi/\text{eV})$. Lowest neutrino mass m_0 has also been assigned with maximum and minimum values of 0.15 eV and 0 respectively.

The cosmological parameters of interest in this paper are the six standard cosmological parameters, effective number of relativistic degrees of freedom N_{eff} , lowest neutrino mass m_0 and effective coupling constant of self-interaction (G_{eff}). The six standard cosmological parameters are: the fraction density of cold dark matter and baryonic matter at present multiplied by square of the reduced Hubble parameter (ω_{cdm} and ω_b respectively), acoustic scale of baryon acoustic oscillation (θ_s), amplitude and the spectral index of the primordial density perturbations (A_s and n_s respectively) and optical depth to the epoch of re-ionization (τ_{reion}). These nine parameters have been varied in this analysis and the corresponding priors for these parameters are given in table 6. We have used Gaussian

Parameter	mean	1- σ
$m_0(\text{eV})$	0.05	0.02
$\log_{10}(m_\phi/\text{eV})$	6.7	0.05
$\log_{10} g_\phi$	-1.5	0.05
γ	2.35	0.05

Table 5: Priors used in MCMC with IceCube data

prior for our purpose. In case of $\log_{10}(G_{\text{eff}})$, we have assigned the maximum and minimum values -5.0 and -0.1 respectively. Lowest neutrino mass m_0 has been varied in the range $[0, 0.2]$ eV and N_{eff} has been varied in the range $[3, 5]$. We have also assigned a minimum value of τ_{reio} at 0.04.

Parameter	mean	1- σ
ω_b	2.2377×10^{-2}	0.015×10^{-2}
ω_{cdm}	0.12010	0.0013
$100\theta_s$	1.04110	3e-4
$\ln(10^{10} A_s)$	3.0447	0.015
n_s	0.9659	0.0042
τ_{reio}	0.0543	0.008
$\log_{10}(G_{\text{eff}})$	-1.5	0.2
m_0	0.008	0.005
N_{eff}	3.75	0.1

Table 6: Priors used in MCMC with Planck, BAO and HST data.

References

- [1] L. Lancaster, F.-Y. Cyr-Racine, L. Knox, and Z. Pan, *A tale of two modes: Neutrino free-streaming in the early universe*, *JCAP* **07** (2017) 033, [[arXiv:1704.06657](#)].
- [2] I. M. Oldengott, T. Tram, C. Rampf, and Y. Y. Wong, *Interacting neutrinos in cosmology: exact description and constraints*, *JCAP* **11** (2017) 027, [[arXiv:1706.02123](#)].
- [3] C. D. Kreisch, F.-Y. Cyr-Racine, and O. Doré, *Neutrino puzzle: Anomalies, interactions, and cosmological tensions*, *Phys. Rev. D* **101** (2020), no. 12 123505, [[arXiv:1902.00534](#)].
- [4] M. Park, C. D. Kreisch, J. Dunkley, B. Hadzhiyska, and F.-Y. Cyr-Racine, *Λ CDM or self-interacting neutrinos: How CMB data can tell the two models apart*, *Phys. Rev. D* **100** (2019), no. 6 063524, [[arXiv:1904.02625](#)].
- [5] G. Barenboim, P. B. Denton, and I. M. Oldengott, *Constraints on inflation with an extended neutrino sector*, *Phys. Rev. D* **99** (2019), no. 8 083515, [[arXiv:1903.02036](#)].
- [6] A. Mazumdar, S. Mohanty, and P. Parashari, *Inflation models in the light of self-interacting sterile neutrinos*, *Phys. Rev. D* **101** (2020), no. 8 083521, [[arXiv:1911.08512](#)].
- [7] N. Blinov and G. Marques-Tavares, *Interacting radiation after Planck and its implications for the Hubble Tension*, *JCAP* **09** (2020) 029, [[arXiv:2003.08387](#)].
- [8] H.-J. He, Y.-Z. Ma, and J. Zheng, *Resolving Hubble Tension by Self-Interacting Neutrinos with Dirac Seesaw*, *JCAP* **11** (2020) 003, [[arXiv:2003.12057](#)].
- [9] A. Das, A. Dighe, and M. Sen, *New effects of non-standard self-interactions of neutrinos in a supernova*, *JCAP* **05** (2017) 051, [[arXiv:1705.00468](#)].
- [10] H. Ko et al., *Neutrino Process in Core-collapse Supernovae with Neutrino Self-interaction and MSW Effects*, *Astrophys. J. Lett.* **891** (2020), no. 1 L24.

- [11] K. Blum, A. Hook, and K. Murase, *High energy neutrino telescopes as a probe of the neutrino mass mechanism*, [arXiv:1408.3799](#).
- [12] N. Blinov, K. J. Kelly, G. Z. Krnjaic, and S. D. McDermott, *Constraining the Self-Interacting Neutrino Interpretation of the Hubble Tension*, *Phys. Rev. Lett.* **123** (2019), no. 19 191102, [[arXiv:1905.02727](#)].
- [13] V. Brdar, M. Lindner, S. Vogl, and X.-J. Xu, *Revisiting neutrino self-interaction constraints from Z and τ decays*, *Phys. Rev. D* **101** (2020), no. 11 115001, [[arXiv:2003.05339](#)].
- [14] K. C. Y. Ng and J. F. Beacom, *Cosmic neutrino cascades from secret neutrino interactions*, *Phys. Rev. D* **90** (2014), no. 6 065035, [[arXiv:1404.2288](#)]. [Erratum: *Phys. Rev. D* **90**, 089904 (2014)].
- [15] A. DiFranzo and D. Hooper, *Searching for MeV-Scale Gauge Bosons with IceCube*, *Phys. Rev. D* **92** (2015), no. 9 095007, [[arXiv:1507.03015](#)].
- [16] I. M. Shoemaker and K. Murase, *Probing BSM Neutrino Physics with Flavor and Spectral Distortions: Prospects for Future High-Energy Neutrino Telescopes*, *Phys. Rev. D* **93** (2016), no. 8 085004, [[arXiv:1512.07228](#)].
- [17] M. Bustamante, C. Rosenstrøm, S. Shalgar, and I. Tamborra, *Bounds on secret neutrino interactions from high-energy astrophysical neutrinos*, *Phys. Rev. D* **101** (2020), no. 12 123024, [[arXiv:2001.04994](#)].
- [18] **Planck** Collaboration, N. Aghanim et al., *Planck 2018 results. VI. Cosmological parameters*, [arXiv:1807.06209](#).
- [19] G. Efstathiou, *H_0 Revisited*, *Mon. Not. Roy. Astron. Soc.* **440** (2014), no. 2 1138–1152, [[arXiv:1311.3461](#)].
- [20] J. L. Bernal, L. Verde, and A. G. Riess, *The trouble with H_0* , *JCAP* **10** (2016) 019, [[arXiv:1607.05617](#)].
- [21] L. Verde, T. Treu, and A. Riess, *Tensions between the early and late universe*, *Nature Astronomy* **03** (Sep, 2019) 891–895, [[arXiv:1907.10625](#)].
- [22] E. Di Valentino et al., *Cosmology Intertwined II: The Hubble Constant Tension*, [arXiv:2008.11284](#).
- [23] A. G. Riess, S. Casertano, W. Yuan, L. M. Macri, and D. Scolnic, *Large Magellanic Cloud Cepheid Standards Provide a 1% Foundation for the Determination of the Hubble Constant and Stronger Evidence for Physics beyond Λ CDM*, *Astrophys. J.* **876** (2019), no. 1 85, [[arXiv:1903.07603](#)].
- [24] K.-F. Lyu, E. Stamou, and L.-T. Wang, *Self-interacting neutrinos: solution to Hubble tension versus experimental constraints*, [arXiv:2004.10868](#).
- [25] F. F. Deppisch, L. Graf, W. Rodejohann, and X.-J. Xu, *Neutrino Self-Interactions and Double Beta Decay*, *Phys. Rev. D* **102** (2020), no. 5 051701, [[arXiv:2004.11919](#)].
- [26] K. Ioka and K. Murase, *IceCube PeV–EeV neutrinos and secret interactions of neutrinos*, *PTEP* **2014** (2014), no. 6 061E01, [[arXiv:1404.2279](#)].
- [27] B. Chauhan and S. Mohanty, *Signature of light sterile neutrinos at IceCube*, *Phys. Rev. D* **98** (2018), no. 8 083021, [[arXiv:1808.04774](#)].
- [28] K. J. Kelly and P. A. Machado, *Multimessenger Astronomy and New Neutrino Physics*, *JCAP* **10** (2018) 048, [[arXiv:1808.02889](#)].
- [29] S. Mohanty, A. Narang, and S. Sadhukhan, *Cutoff of IceCube Neutrino Spectrum due to t -channel Resonant Absorption by $C\nu B$* , *JCAP* **03** (2019) 041, [[arXiv:1808.01272](#)].
- [30] C. Creque-Sarbinowski, J. Hyde, and M. Kamionkowski, *Resonant Neutrino Self-Interactions*, [arXiv:2005.05332](#).
- [31] Y. Chikashige, R. N. Mohapatra, and R. Peccei, *Are There Real Goldstone Bosons Associated with Broken Lepton Number?*, *Phys. Lett. B* **98** (1981) 265–268.
- [32] G. Gelmini and M. Roncadelli, *Left-Handed Neutrino Mass Scale and Spontaneously Broken Lepton Number*, *Phys. Lett. B* **99** (1981) 411–415.

- [33] H. M. Georgi, S. L. Glashow, and S. Nussinov, *Unconventional Model of Neutrino Masses*, *Nucl. Phys. B* **193** (1981) 297–316.
- [34] G. B. Gelmini, S. Nussinov, and M. Roncadelli, *Bounds and Prospects for the Majoron Model of Left-handed Neutrino Masses*, *Nucl. Phys. B* **209** (1982) 157–173.
- [35] S. Nussinov and M. Roncadelli, *Observable Effects of Relic Majorons*, *Phys. Lett. B* **122** (1983) 387–391.
- [36] U. K. Dey, N. Nath, and S. Sadhukhan, *Charged Higgs effects in IceCube: PeV events and NSIs*, [arXiv:2010.05797](#).
- [37] F. Arias-Aragon, E. Fernandez-Martinez, M. Gonzalez-Lopez, and L. Merlo, *Neutrino Masses and Hubble Tension via a Majoron in MFV*, [arXiv:2009.01848](#).
- [38] M. Berbig, S. Jana, and A. Trautner, *The Hubble tension and a renormalizable model of gauged neutrino self-interactions*, [arXiv:2004.13039](#).
- [39] I. Esteban, M. Gonzalez-Garcia, M. Maltoni, T. Schwetz, and A. Zhou, *The fate of hints: updated global analysis of three-flavor neutrino oscillations*, [arXiv:2007.14792](#).
- [40] H. Goldberg, G. Perez, and I. Sarcevic, *Mini Z' burst from relic supernova neutrinos and late neutrino masses*, *JHEP* **11** (2006) 023, [[hep-ph/0505221](#)].
- [41] Y. Farzan and S. Palomares-Ruiz, *Dips in the Diffuse Supernova Neutrino Background*, *JCAP* **06** (2014) 014, [[arXiv:1401.7019](#)].
- [42] C.-P. Ma and E. Bertschinger, *Cosmological perturbation theory in the synchronous and conformal Newtonian gauges*, *Astrophys. J.* **455** (1995) 7–25, [[astro-ph/9506072](#)].
- [43] S. Hannestad and R. J. Scherrer, *Selfinteracting warm dark matter*, *Phys. Rev. D* **62** (2000) 043522, [[astro-ph/0003046](#)].
- [44] F. Forastieri, M. Lattanzi, G. Mangano, A. Mirizzi, P. Natoli, and N. Saviano, *Cosmic microwave background constraints on secret interactions among sterile neutrinos*, *JCAP* **07** (2017) 038, [[arXiv:1704.00626](#)].
- [45] N. Song, M. Gonzalez-Garcia, and J. Salvado, *Cosmological constraints with self-interacting sterile neutrinos*, *JCAP* **10** (2018) 055, [[arXiv:1805.08218](#)].
- [46] I. M. Oldengott, C. Rampf, and Y. Y. Y. Wong, *Boltzmann hierarchy for interacting neutrinos I: formalism*, *JCAP* **04** (2015) 016, [[arXiv:1409.1577](#)].
- [47] A. Das and S. Ghosh, *Flavor-specific Interaction Favours Strong Neutrino Self-coupling*, [arXiv:2011.12315](#).
- [48] J. Lesgourgues, *The Cosmic Linear Anisotropy Solving System (CLASS) I: Overview*, [arXiv:1104.2932](#).
- [49] B. Audren, J. Lesgourgues, K. Benabed, and S. Prunet, *Conservative Constraints on Early Cosmology: an illustration of the Monte Python cosmological parameter inference code*, *JCAP* **1302** (2013) 001, [[arXiv:1210.7183](#)].
- [50] **Planck** Collaboration, Y. Akrami et al., *Planck 2018 results. X. Constraints on inflation*, [arXiv:1807.06211](#).
- [51] **BOSS** Collaboration, S. Alam et al., *The clustering of galaxies in the completed SDSS-III Baryon Oscillation Spectroscopic Survey: cosmological analysis of the DR12 galaxy sample*, *Mon. Not. Roy. Astron. Soc.* **470** (2017), no. 3 2617–2652, [[arXiv:1607.03155](#)].
- [52] A. Lewis, *GetDist: a Python package for analysing Monte Carlo samples*, [arXiv:1910.13970](#).
- [53] M. Ahlers, L. A. Anchordoqui, and S. Sarkar, *Neutrino diagnostics of ultra-high energy cosmic ray protons*, *Phys. Rev. D* **79** (2009) 083009, [[arXiv:0902.3993](#)].
- [54] S. Ando and K. Sato, *Relic neutrino background from cosmological supernovae*, *New J. Phys.* **6** (2004) 170, [[astro-ph/0410061](#)].

- [55] S. Horiuchi, J. F. Beacom, and E. Dwek, *The Diffuse Supernova Neutrino Background is detectable in Super-Kamiokande*, *Phys. Rev. D* **79** (2009) 083013, [[arXiv:0812.3157](#)].
- [56] **IceCube** Collaboration, C. Kopper, *Observation of Astrophysical Neutrinos in Six Years of IceCube Data*, *PoS ICRC2017* (2018) 981.
- [57] W. Hastings, *Monte Carlo Sampling Methods Using Markov Chains and Their Applications*, *Biometrika* **57** (1970) 97–109.
- [58] R. Barlow, *Asymmetric statistical errors*, in *Statistical Problems in Particle Physics, Astrophysics and Cosmology*, pp. 56–59, 6, 2004. [physics/0406120](#).